Journal of Visualization, Vol. 8, No. 1 (2005)73-81

A Numerical Study on the Enhancement of Heat Transfer by Pressure Distributions in Acoustic Fields

Oh, Y. K.*[1] and Yang, H. D.*[2]

*1 Department of Mechatronics Engineering, Chosun University, 375 Seosuk-dong, Dong-gu, Gwangju 501-759, Korea. E-mail: ygoh@mail.chosun.ac.kr
*2 Department of Precision Mechanical Engineering, The Graduate School of Chosun University, 375 Seosuk-dong, Dong-gu, Gwangju 501-759, Korea.

Received 25 July 2003
Revised 18 October 2004

Abstract : The enhancement of heat transfer in a cavity was investigated in the absence of and in the presence of acoustic streaming induced by ultrasonic waves. The present study provides the experimental and numerical results of heat transfer in the acoustic fields. The enhancement of heat transfer was experimentally investigated in the presence of acoustic streaming and was compared with the profiles of acoustic pressure calculated by the numerical analysis. A coupled finite element-boundary element method (FE-BEM) was applied for a numerical analysis. Experimental and numerical studies clearly show that pressure variations are closely related to the enhancement of heat transfer in the acoustic fields.

Keywords : Acoustic pressure, Acoustic streaming, Particle imaging velocimetry (PIV), Coupled FE-BEM, Ultrasonic wave.

1. Introduction

In some heat transfer problems, phase change (i.e. melting or solidification) frequently occurs. Some common examples include the thermal energy storage system using a latent heat of phase change material, metallurgical processes such as welding and casting and the materials science applications such as crystal growth. The effective augmentation technique of heat transfer is now required because of the practical importance of this subject. The effects of ultrasonic waves in the liquid have been studied by several researchers (Iida et. al., 1991), (Frenkel et. al., 2001), (Oh et. al., 2001). Applying ultrasonic waves in a medium may cause the flow velocity of the medium to increase: an effect known as acoustic streaming (Frenkel et al., 2001). It has been reported that acoustic streaming promotes heat transfer through convection and affects the thermal boundary layer. Actually, Oh and Park (2002) reported that acoustic streaming could develop thermally-oscillating flow and enhance heat transfer during the melting process of paraffin. Figures 1 and 2 show the two-dimensional velocity fields and thermally-oscillating flow for each case with the ultrasonic waves and without the ultrasonic waves which were measured by Oh and Park (2002). It is speculated that acoustic pressure may be closely related to the effect of augmentation of local heat transfer, judging from the facts that applying ultrasonic waves to the liquid medium gives rise to areas of high and low local pressure. Therefore, the objective of the present study is to establish the relationship between the local heat transfer and pressure distributions in acoustic fields.

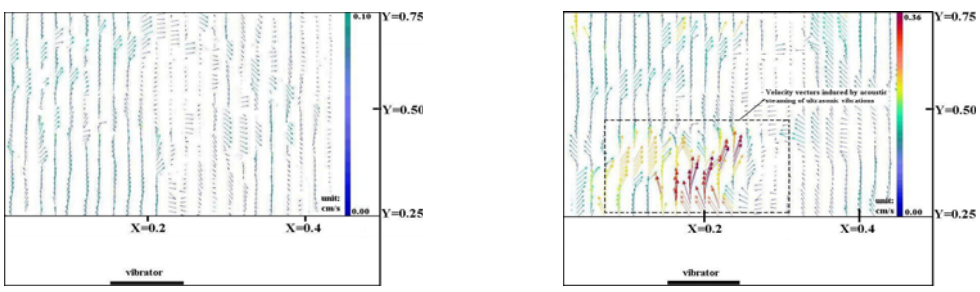

(a) Melting without ultrasonic vibrations (b) Melting with ultrasonic vibrations

Fig. 1. Two dimensional velocity profiles at the visualization window.

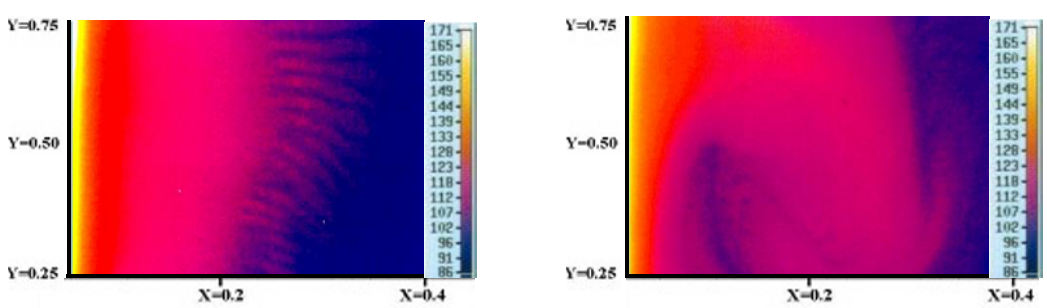

(a) Melting without ultrasonic vibrations (b) Melting with ultrasonic vibrations

Fig. 2. The development of thermally-oscillating flow by acoustic streaming.

2. Experiments

Paraffin (n-octadecane) with the melting point of 53.2ºC was selected as a medium because it is commonly used in a thermal-energy storage system. Thermophysical properties of liquid paraffin are listed in Table 1. Experiments were conducted in a melting cavity after the completion of the melting of solid paraffin as shown in Fig. 3(a). The cavity had inner dimensions of 13 cm×12.5 cm×12.5 cm (height×length×width). A stainless-steel plate heater was vertically positioned on the left side of the cavity, providing a constant heat flux, q"=6433.13 W/m^2 regulated by an automatic voltage regulator (AVR) during the melting process. Generally, the physical properties of the paraffin changed when temperature increased above 200°C because the continuous chains of carbon atoms began to break up at that temperature (Hong, 1990). Therefore, it was necessary to keep the heater temperature below 200°C. To achieve that, we used the heat flux of 6433.13 W/m^2 under which the heater surface temperature was kept below 200°C. To obtain a constant heat flux condition, a plate heater was heated electrically by an automatic voltage regulator, which was designed to maintain a constant output voltage to within ± 1%, with an input voltage variation of ± 20%.

Table 1. Thermophysical properties of liquid paraffin.

Properties	Value
Melting Temperature	53.2 °C
Thermal Conductivity	0.210 W/m·K
Density	863.03 kg/m^3
Specific Heat	2,873 J/kg· K
Viscosity	0.00028 m^2/s
Heat of Fusion	241.60 kJ/kg
Thermal Expansion Coefficient	0.001

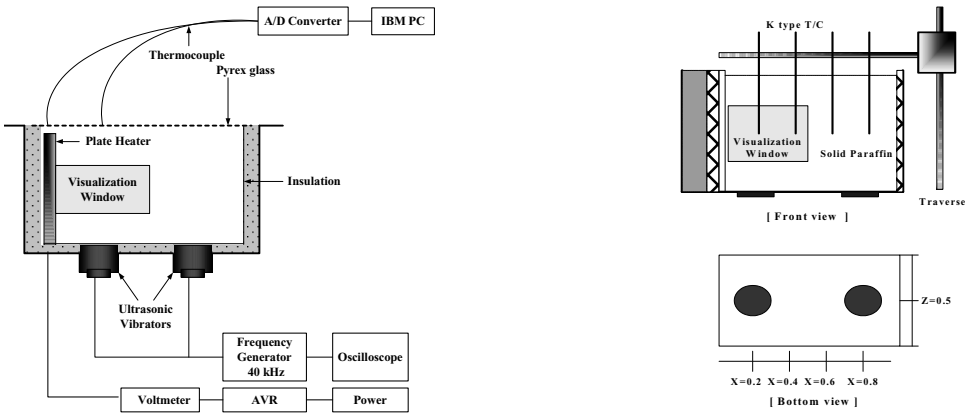

(a) Experimental set-up

(b) Test section for showing the position of ultrasonic transducers and thermocouples

Fig. 3. Schematic diagram of the present experimental set-up.

Two ultrasonic transducers are installed at two axial locations (i.e., X=0.2 and X=0.8) as shown in Fig. 3(b). The resonance frequency of 40kHz was applied from frequency generator to two ultrasonic transducers. The back of the heater surface was insulated with a bakelite plate and fiberglass so that the heat would propagate from the heater surface to the direction of the liquid. In addition, all four outside walls of the cavity were covered with styrofoam and fiberglass plate for insulation purposes. Four chromel-alumel thermocouples of 15cm length were installed at pre-selected locations (X =0.2, 0.4, 0.6, 0.8, and Z=0.5) by using a traverse which can be controlled the accurate position to 0.5mm. Each thermocouple was wound in an insulation tape and was sheathed in a stainless-steel tube except at the junction to minimize heat conduction from a connecting thermocouple wire to the liquid. Before the experiments, all thermocouples were calibrated with a calibration voltage source. The melting tests were carried out three times under the same condition in order to ensure the accurate temperature distributions. The largest temperature deviations from the average temperature were about ± 5°C on the heater and about ± 2°C in the liquid paraffin. A particle imaging velocimetry was used for the visualization of flow fields through a visualization window. Also, in the present study, a fixed frequency level of 40kHz was selected, but power levels were varied from 70 to 340 W in order to investigate the effect of the strength ultrasonic vibrations on heat and mass transfer.

3. Numerical Analysis

High frequency vibration of the excited plate radiates ultrasonic waves to the liquid paraffin and causes acoustic pressure in the liquid. Basically, the acoustic pressure in the liquid can be experimentally measured using a hydrophone. However, it is impossible to measure the accurate pressure using a hydrophone when the liquid is heated over 120°C. In the present study, the liquid paraffin in a cavity was heated over 135°C under a constant heat flux condition. Therefore, numerical analysis was applied to calculate the acoustic pressure in the liquid paraffin instead of the experimental measurement. For the numerical analysis, SVS[1](Structural Vibration Sound) programmed with Fortran language and based on a coupled FE-BEM was used in the present study.

Figure 4 shows a finite element, finite-meshes and fixed boundary condition of vibrating plate

[1] SVS is a commercial FE-BEM package which was developed and programmed by Dr. Jarng, who is a professor of Chosun University.

for a coupled FE-BEM. As shown in Fig. 4(a), each element node was rearranged to follow the SVS element array after ANSYS™ finite element modeling. Each element is composed of 20 quadratic nodes and each surface boundary has 8 quadratic nodes. Figure 4(b) shows a finite element meshes for a vibrating plate, including two ultrasonic transducers. The element size of the numerical model does not exceed about 4.2 mm, which is about 1/6 of the wavelength of 40 kHz waves in order to assure the accuracy of the numerical analysis. Figure 4(c) shows fixed boundary conditions of a vibrating plate where all elements are fixed two ultrasonic transducers.

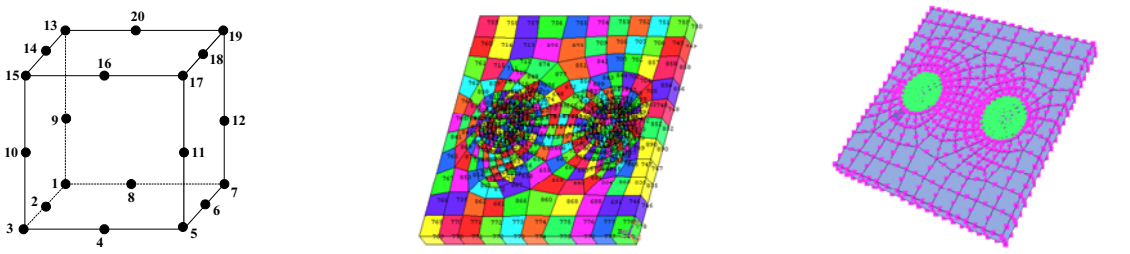

(a) Element of composed 20 nodes (b) Finite-element meshes (c) Fixed boundary condition

Fig. 4. Schematic diagram of a modeling for the numerical analysis.

4. Results and discussions

4.1 The PIV measurement

The PIV observation clearly shows that the application of the ultrasonic waves to the liquid initiates a strong upward flow, acoustic streaming. Basically, there are two types of acoustic streaming. The first, which has received the majority of attention to date, is Rayleigh streaming. This is caused by relative oscillatory motion between the fluid and a boundary. The steady flow results from the rapid change in the wave amplitude in the acoustic boundary layer. The effects of attenuation are usually considered to be negligible. The second, Eckart streaming, results from the attenuation of the wave in the bulk fluid. Here the momentum transfer from the wave is converted into a time-averaged flow moving away from the source (Haydock and Yeomans, 2001). According to the above classifications, the acoustic streaming observed in Figs. 5(a), 6(a) and 7(a) is close to quasi-Eckart streaming which can generate an intense fluid motion. This flow seems to increase heat and mass transfer, destroying the flow instability.

In the present study, the output power level at a frequency generator was adjusted to investigate the effect of ultrasonic intensity on heat transfer. Figures 5, 6 and 7 show the velocity fields and kinetic energy distributions induced by ultrasonic waves when the output power levels varied from 70 W to 340 W.

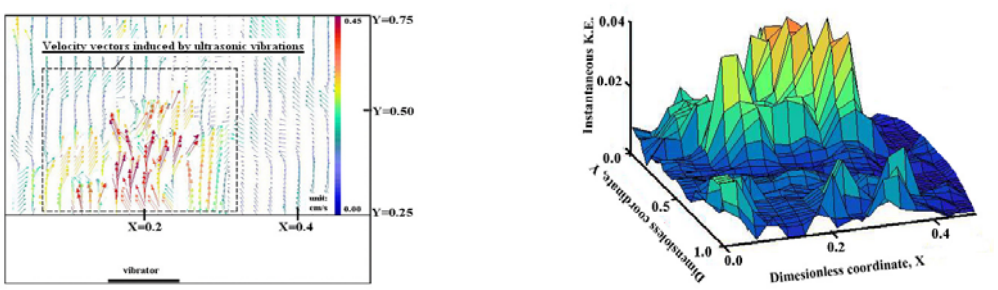

(a) Velocity profiles (b) Kinetic energy distribution

Fig. 5. Two dimensional velocity profiles and kinetic energy distribution at the output power level of 340 W.

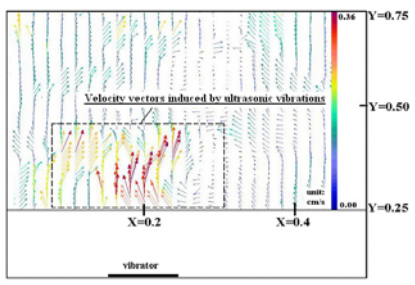

(a) Velocity profiles

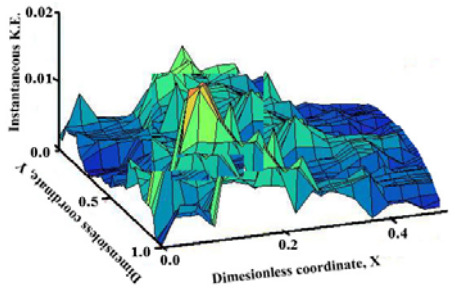

(b) Kinetic energy distribution

Fig. 6. Two dimensional velocity profiles and kinetic energy distribution at the output power level of 185 W.

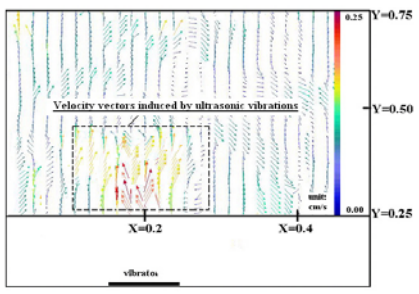

(a) Velocity profiles

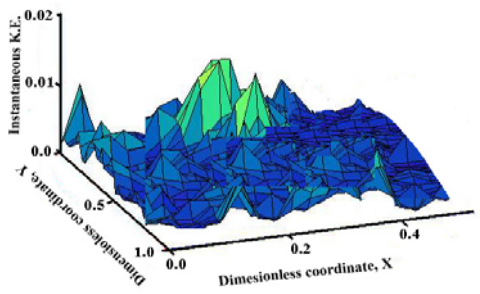

(b) Kinetic energy distribution

Fig. 7. Two dimensional velocity profiles and kinetic energy distribution at the output power level of 70 W.

For each case, the upward flow initiated from the point where the ultrasonic transducer is installed (i.e., dimensionless coordinate X=0.2). At the higher output power level, more intensive flow motions are developed. Due to a strong upward flow (i.e., quasi-Eckart flow), kinetic energy is increased with increasing the output power level as shown in Figs. 5-7. This fluid dynamics is believed to increase the heat and mass transfer.

4.2 The augmentation ratio of heat transfer

In order to evaluate the rate of heat transfer enhancement, total consumed electricity was measured for the following two cases: melting with a heater only, and melting with both heater and ultrasonic vibrations to investigate the efficiency of energy as the quantity of heat transfer enhancement when the ultrasonic waves were applied during the melting process. Table 2 shows the melting times when the output power levels varied from 70 to 340W. The higher the output power level was, the faster the melting speed was. Moreover, as shown in Table 3, the total consumed electricity for the case with a heater and ultrasonic vibrations was saved about 2.2～2.8 Wh as compared with the case with a heater only. That is, energy can be clearly saved by using ultrasonic vibrations. These results help to evaluate the rate of heat transfer enhancement.

Table 2. Melting time under variable output power level.

Heat flux [W/m^2]	Output power level [W]	Melting time [Min]
6433.13	340	72
	185	94
	70	164

Table 3. Comparison of the total consumed electricity under the output power level of 185W.

Heat flux 6433.13 [W/m²]	Melting time [Min]	Consumed electricity at Heater [Wh]	Total consumed electricity [Wh]
Without ultrasonic vibrations	275	444.6	444.6
With ultrasonic vibrations	94	152.0	441.8

Local heat transfer coefficient in the liquid can be calculated from:

$$h = \frac{q''}{T_h - T_\infty} \tag{1}$$

Where, q'' is the heat flux, T_h is the heater surface temperature and T_∞ is the liquid temperature of selected location which was measured by using a thermocouples. In the end, the augmentation ratio of heat transfer (Δh) in the liquid can be defined as following:

$$\Delta h = h / h_0 \tag{2}$$

Where, h is the heat transfer coefficient with ultrasonic vibrations and h_0 is one without ultrasonic vibrations.

4.3 Acoustic pressure distributions in the liquid region

The acoustic pressure $p(r,t)$ caused by the wave propagation in a non-viscous compressible fluid is governed by the following wave equation.

$$\nabla^2 p - \frac{1}{c^2}\frac{\partial^2 p}{\partial t^2} = 0 \tag{3}$$

Where, r and t are the space and time coordinates, respectively. ∇^2 is Laplacian and c is the wave speed. In general, the wave speed and density in a medium are proportional to the temperature of a medium. Therefore, in the present study, a fixed average temperature (130°C) which is generally used in a heating problem was considered. The average temperature of a medium can be calculated from (Hong, 1990), (Mashiro, 1995):

$$T_{avg} = \frac{1}{2}(T_h + T_\infty) \tag{4}$$

For the density estimation, the following relation which a paraffin manufacturer, Shinyo Pure Chemical Co. provided was used.

$$\rho = 778.3 \exp[-8.249 \times 10^{-4}(T - 50)] \tag{5}$$

The wave velocity, v in a medium was obtained by relating the results from Eqs. (4) and (5) to the following equation.

$$v = \sqrt{\frac{E}{\rho}} = \sqrt{\frac{1}{k_T \rho}} \tag{6}$$

Where, E and k_T is bulk modulus and compressibility, respectively. The Bulk modulus of the liquid

Table 4. Bulk modulus of elasticity of paraffin (n-octadecane).

Temperature	Bulk modulus of elasticity (N/m²)	
	1 atm	100 atm
60.0	1.06×10^9	1.96×10^9
79.4	9.61×10^8	1.82×10^9
98.9	8.62×10^8	1.72×10^9
115.0	7.81×10^8	1.64×10^9
135.0	6.94×10^8	1.56×10^9

paraffin between 1 atm and 100 atm listed in Table 4 come from CRC handbook of chemistry and physics (Cutler et al., 1958).

4.4 The comparison of experimental and numerical result

In Fig. 8, the augmentation effect of heat transfer experimentally measured was compared with the acoustic pressure obtained by numerical prediction when ultrasonic intensity varied from 70 W to 340 W.

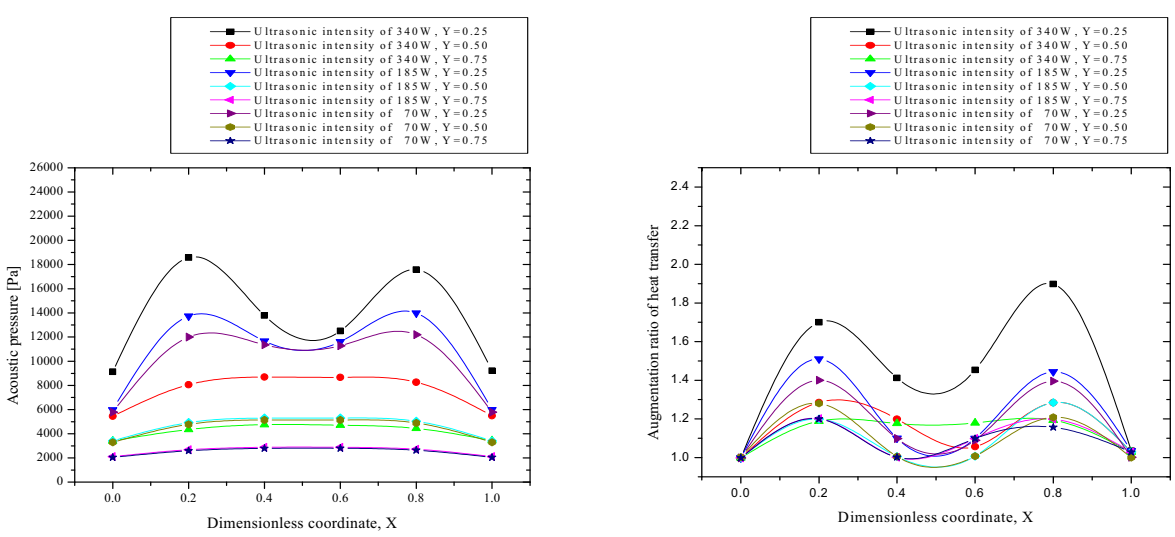

(a) Acoustic pressure distributions (b) Augmentation ratio of local heat transfer

Fig. 8. Comparison between the acoustic pressure distribution and augmentation ratio of local heat transfer in each case of ultrasonic intensity and dimensionless coordinate Y.

As shown in Fig. 8(a), the acoustic pressure is higher at the points where two ultrasonic transducers (i.e., X=0.2 and X=0.8) are installed than other points. Particularly, at the dimensionless coordinate, Y=0.25 and X=0.2 and 0.8, the acoustic pressure reveals the maximum value for three different ultrasonic intensities. These points are in a good agreement with points where the kinetic energy distribution is higher (see Figs. 5, 6 and 7). However, in case of Y > 0.25, the value of acoustic pressure is almost same because acoustic wave uniformly propagates through the whole liquid region as shown in Fig. 9. Figure 9 visually shows that pressure variations result in a liquid paraffin with the ultrasonic vibrations calculated by numerical analysis.

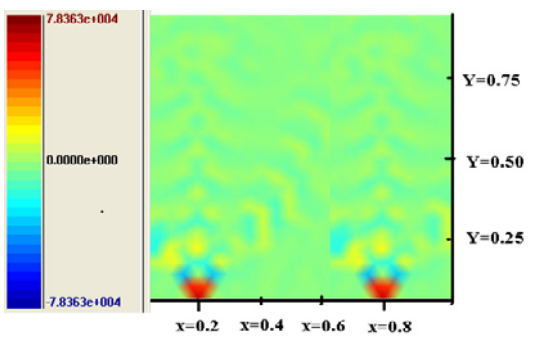

Fig. 9. Two dimensional acoustic pressure distributions calculated by a coupled FE-BEM.

Figure 8(b) shows the augmentation ratio of heat transfer that was plotted by the equation (2). It is also higher at the points where two ultrasonic transducers are installed because the strong ultrasonic waves cause the flow velocity of the liquid to increase and promote heat transfer as revealed in the PIV measurement. Although the profiles between the acoustic pressure and heat transfer augmentation are not exactly matched and rather irregular for each other, they still have a similar pattern. In Table 5, the calculated the augmentation ratio of heat transfer and acoustic pressure during the ultrasonic intensities varied from 70W to 340W are listed with respect to dimensionless coordinates. As shown in Table 5, an increase in the acoustic pressure can enhance the ratio of heat transfer. From these results, we can conclude that the acoustic pressure caused by ultrasonic waves initiates a strong flow motion such as Eckart streaming which helps to increase the local heat transfer.

Table 5. Acoustic pressure and the augmentation ratio of heat transfer for three different ultrasonic intensities.

Power [W]	X	Acoustic pressure [Pa]			Augmentation ratio of heat transfer		
		Y=0.25	Y=0.50	Y=0.75	Y=0.25	Y=0.50	Y=0.75
340	0.0	9,137	5,453	3,413	0.998	0.998	0.998
	0.2	18,579	8,058	4,355	1.700	1.285	1.188
	0.4	13,789	8,690	4,756	1.412	1.199	1.176
	0.6	12,505	8,667	4,708	1.453	1.056	1.179
	0.8	17,582	8,264	4,446	1.898	1.284	1.193
	1.0	9,217	5,484	3,427	1.035	1.029	1.028
185	0.0	5,985	3,408	2,111	0.998	0.998	0.998
	0.2	13,735	4,924	2,677	1.510	1.199	1.201
	0.4	11,665	5,298	2,884	1.100	1.005	1.001
	0.6	11,618	5,305	2,888	1.099	1.007	1.098
	0.8	13,988	5,041	2,727	1.444	1.284	1.199
	1.0	5,994	3,410	2,112	1.035	1.029	1.028
70	0.0	5,782	3,298	2,044	0.998	1.002	0.998
	0.2	12,000	4,779	2,594	1.400	1.280	1.200
	0.4	11,361	5,146	2,797	1.098	1.005	1.001
	0.6	11,279	5,149	2,800	1.089	1.007	1.098
	0.8	12,201	4,891	2,644	1.395	1.208	1.156
	1.0	5,783	3,299	2,045	1.001	1.000	1.028

5. Conclusion

The profiles of the augmentation ratio of heat transfer coefficient were experimentally measured and were compared with those of the acoustic pressure obtained by numerical prediction in the liquid when the ultrasonic waves were applied. The heat transfer coefficient increases with increase in the ultrasonic intensities. The largest augmentation ratio of heat transfer (about 27.6%) is measured at the ultrasonic intensity of 340W. Also, the results of numerical analysis show the acoustic pressure increase about 60.4%, 38.8% and 35.3% at the ultrasonic intensity of 340W, 185W and 70W, respectively. Consequently, this study offers significant evidence that an intense flow motion induced by ultrasonic waves can affect heat and mass transfer. This phenomenon, which is called acoustic streaming, obviously revealed by the PIV measurement leads to increase in the velocity and the kinetic energy of a fluid which is a crucial physical concept to explain the augmentation of convective heat transfer. Also, acoustic streaming results from sudden acoustic pressure variations in the liquid.

The higher acoustic pressure distribution near two ultrasonic transducers develops more intensive flow (quasi-Eckart streaming) motion, destroying the flow instability. The profile of the acoustic pressure variation is consistent with that of augmentation of heat transfer. In the end, this mechanism is believed to increase the ratio of heat transfer coefficient.

Acknowledgment

This study was supported by a research funds from Chosun University, 2004.

References

Cutler, W. G., McMickle, R. H., Webb, W. and Schiessler, R. W., J. Chem. Phys., 29 (1958), 727.
Frenkel, V., Gurka, L. and Shavit, U., Preliminary Investigations of Ultrasonic induced Acoustic Streaming using Particle Image Velocimetry, Ultrasonics, 39 (2001), 153-156.
Haydock, D.and Yeomans, J. M., Lattice Boltzmann Simulations of Acoustic Streaming, J. Phys. A, Math. Gen, 34 (2001), 5201-5213.
Hong, J. S., Studies on Heat Storing and Retrieving Characteristics in a Paraffin-Filled Horizontal Circular Tube, Ph. D. Thesis, Seoul National Univ., Korea, 1990.
Iida, Y., Tsutsui, K., Ishii, R. and Yamada, Y., Natural Convection Heat transfer in a Field of Ultrasonic Waves and Sound Pressure, Journal of Chemical Engineering of Japan, 24 (1991), 794-796.
Jarng, S. S., Sonar Transducer Analysis Using a Coupled FE-BE Method, Proc. of the 12 Korea Automatic Control Conf., 12 (1997), 1750-1753.
Mashiro, Heat Transfer, Korean ed., Sigma Press, Seoul, Korea, (1995), 200-201.
MacCollum, M. D. and Clementina, M. S., Modal Analysis of a Structure in a Compressible Fluid Using a Finite Element/Boundary Element Approach, J. Acoust. Soc. 99 (1996), 1949-1957.
Oh, Y. K., Park, S. H. and Cha, K. O., An Experimental Study of Accelerating Phase Change Heat Transfer", KSME International Journal, 15 (2001), 1882-1891.
Oh, Y. K. and Park, S. H., Acoustic Enhancement of Solid-Liquid Phase Change Heat Transfer, Journal of Energy Eng. 11-3 (2002), 262-268.

Author Profile

Yool Kwon Oh: He received his M.Sc. (Eng) degree in Mechanical Engineering in 1981 from Hanyang University. He also received his Ph.D in Mechanical Engineering in 1991 from Kyunghee University. He worked in Department of Mechanical Engineering, Illinois University as a visiting professor from 1986 to 1987 and Drexel University as a visiting professor from 1995 to 1996. He works in Department of Mechatronics Engineering of Chosun University as a professor since 1981. His research interests are Thermodynamics, Steam Power Plant and Internal Combustion Engine, Heat and Fluid Analysis, Solar Energy and Phase Change Heat Transfer in Acoustic Fields.

Ho Dong Yang: He received his bachelor degree in Mechanical Engineering from Chosun University in 2003. He entered into Department of Precision Mechanical Engineering in the graduate school of hosun University in 2003. He works in Thermal Engineering Laboratory and Research Assistant. His current research interests are Enhancement of Heat Transfer in Acoustic Fields by using the Ultrasonic Vibration and Computational Simulation of Thermal-Fluid Dynamics.